Exp Brain Res (2015) 233:3187–3200
DOI 10.1007/s00221-015-4387-5

RESEARCH ARTICLE

Neural mechanisms underlying the exploration of small city maps using magnetoencephalography

Sofia Sakellaridi[1,2,3] · Peka Christova[2,4] · Vassilios Christopoulos[5] · Arthur C. Leuthold[2,4] · John Peponis[6] · Apostolos P. Georgopoulos[1,2,4]

Received: 30 December 2014 / Accepted: 11 July 2015 / Published online: 8 August 2015

Abstract The neural mechanisms underlying spatial cognition in the context of exploring realistic city maps are unknown. We conducted a novel brain imaging study to address the question of whether and how features of special importance for map exploration are encoded in the brain to make a spatial decision. Subjects explored by eyes small city maps exemplifying five different street network types in order to locate a hypothetical City Hall, while neural activity was recorded continuously by 248 magnetoencephalography (MEG) sensors at high temporal resolution. Monitoring subjects' eye positions, we locally characterized the maps by computing three spatial parameters of the areas that were explored. We computed the number of street intersections, the total street length, and the regularity index in the circular areas of 6 degrees of visual angle radius centered on instantaneous eye positions. We tested the hypothesis that neural activity during exploration is associated with the spatial parameters and modulated by street network type. All time series were rendered stationary and nonautocorrelated by applying an autoregressive integrated moving average model and taking the residuals. We then assessed the associations between the prewhitened time-varying MEG time series from 248 sensors and the prewhitened spatial parameters time series, for each street network type, using multiple linear regression analyses. In accord with our hypothesis, ongoing neural activity was strongly associated with the spatial parameters through localized and distributed networks, and neural processing of these parameters depended on the type of street network. Overall, processing of the spatial parameters seems to predominantly involve right frontal and prefrontal areas, but not for all street network layouts. These results are in line with findings from a series of previous studies showing that frontal and prefrontal areas are involved in the processing of spatial information and decision making. Modulation of neural processing of the spatial parameters by street network type suggests that some street network layouts may contain other types of spatial information that subjects use to explore maps and make spatial decisions.

Keywords Spatial decision making · Eye fixations · Map reading · Magnetoencephalography

✉ Apostolos P. Georgopoulos
omega@umn.edu

[1] Center for Cognitive Sciences, University of Minnesota, Minneapolis, MN, USA

[2] Brain Sciences Center (11B), Veterans Affairs Medical Center, VAHCS, One Veterans Drive, Minneapolis, MN 55417, USA

[3] Present Address: Department of Neurobiology, University of California Los Angeles, Los Angeles, CA, USA

[4] Department of Neuroscience, University of Minnesota Medical School, Minneapolis, MN, USA

[5] Division of Biology and Biological Engineering, California Institute of Technology, Pasadena, CA, USA

[6] School of Architecture, College of Architecture, Georgia Institute of Technology, Atlanta, GA, USA

Introduction

The ability to make spatial decisions while exploring an environment is a fundamental component of human and animal behavior and very critical for survival. For instance, animals in nature explore their surroundings to obtain food, avoid predators, and find mates. Similarly, people frequently explore new environments to find places for food and entertainment, buy new houses, etc. These problems

involve some aspects of spatial information processing in which humans/animals extract spatial information from the environment to combine it with other decision variables, internal states (e.g., hunger level), and external states (e.g., threat level) to make decisions. The question of how people and animals extract and process spatial information for making decisions is a topic of many ongoing studies.

For years, scientists have strived to understand how we interact with our environment to collect information required to make decisions or to select actions. One of the studies that aimed to address this question involved a maze solving task (Crowe et al. 2000), in which individuals were presented with a maze stimulus on a video display and had to indicate which of several possible exits from the maze was continuous with a specific entrance. The results showed that reaction time was positively correlated with the length of the main path, the number of turns in the path, and the direct distance from the entry to the endpoint. Additionally, gaze behavior and eye fixations were also modulated by spatial characteristics of the mazes. Similar results were reported in a maze solving experiment with nonhuman primates (Chafee et al. 2002). These findings suggest that: (1) People and animals can solve mazes in a similar fashion, (2) the postulated dynamic spatial process involves a mental tracing of the maze path, and (3) a significant aspect of the spatial information processing involves the length and turns of the path.

Although these studies provide important knowledge on which and how spatial information is processed during exploration tasks, mazes were randomly generated and restricted. A recent study extended the maze solving task using small city maps as stimuli (Christova et al. 2012). According to this study, people had to explore continuously realistic small city maps of various US cities by moving their eyes, in order to select a location to build a hypothetical City Hall. Unlike the maze solving task, this study involved both exploration and spatial decision making. Hence, people had to collect spatial information not to find a path to a goal, but to identify a location for building the City Hall. Results showed that people chose City Hall locations with very similar spatial attributes—i.e., placed City Hall at some of the most accessible locations within each city map.

These findings suggest that people and animals use particular spatial information from the environment to solve spatial-context problems and make decisions. However, little is known about the neural mechanism underlying spatial information processing in this context. Recent functional imaging studies explored the characteristics of the brain networks that are involved in exploration and navigation. In particular, humans were trained to explore and navigate in novel environments, while brain activity was measured using fMRI. The results revealed a widespread network of brain structures that include subcortical (e.g., hippocampus and parahippocampal gyrus), as well as cortical (e.g., premotor cortex, posterior parietal cortex, posterior cingulate cortex) regions that are involved in spatial exploration and navigation (Aguirre et al. 1996; Maguire et al. 1998; Spiers and Maguire 2006, 2007). Despite the significant knowledge gained by these studies, they are limited by the low temporal resolution of fMRI. Moreover, they do not address the question of how information that is required to make spatial decisions is encoded in the brain. In the current study, we take advantage of the high temporal resolution of the MEG to study how the brain encodes spatial information, while humans explore novel environments to make spatial decisions. To do that, we conducted a novel brain imaging experiment, in which subjects were instructed to explore by eyes various US city maps exemplifying five different street network types, i.e., regular, colliding, curvilinear, cul-de-sac, and supergrid, in order to select a location to build a hypothetical City Hall. We recorded neuromagnetic fluxes from subjects' heads using a 248-sensor whole-head magnetoencephalography device. We also monitored subjects' eye positions to locally characterize the maps by computing three spatial attributes in the circular area of 6 degrees of visual angle (DVA) radius centered on each eye position (i.e., covertly explore area): (a) the total street length, (b) the number of street intersections, and (c) the regularity index that measures the degree to which the distribution of street intersections deviates from complete spatial randomness to either clustering or regularity. We call these attributes *space syntax parameters*, because we quantified them using space syntax analysis—i.e., a set of analytic techniques that are used to describe the average properties of a street network over an area (Hillier 1996; Peponis and Wineman 2002).

The hypothesis was that some or all of these space syntax parameters are encoded in the brain through characteristic neuronal networks, and neural processing of these parameters is modulated by street network type. We assessed the relation between the time-varying MEG signals from the 248 sensors with the variability of each of the space syntax parameters, for each street network type, using MLR analyses. In accord with our hypothesis, ongoing neural activity was strongly associated with space syntax parameters through localized and distributed networks, and the neural processing of these parameters was modulated by the type of street network. To the best of our knowledge, this is the first study showing how the brain encodes spatial information during map exploration for making spatial decisions.

Materials and methods

Subjects

Ten right-handed subjects (five women and five men, all of them living in the USA for more than 7 years) participated in the study for monetary compensation. Subjects' age ranged from 21 to 60 years (women's age 32 ± 12.1 years, mean ± SEM; men's age 38.6 ± 13.2 years). The age did not differ significantly between sexes ($P = 0.18$, t test). The appropriate institutional review board approved the study protocol, and the informed consent was obtained from all the participants based on the Declaration of Helsinki.

Stimuli

In the current study, we used the same stimuli from the previous study conducted in our laboratory (Christova et al. 2012). Stimuli were circular maps of 3-mile diameter urban areas extracted from street centerline maps and represent several US Metropolitan Statistical Areas (Atlanta, GA; Baltimore, MD; Chicago, IL; Los Angeles, CA; New York, NY; Pittsburgh, PA; St. Louis, MO; Tampa, FL; Washington, DC). Street centerline maps show information about the position of streets relative to one another, scaled length, sinuosity, alignment, and pattern of intersections of the street network. The sample was chosen to exemplify five different street networks types, namely (1) *regular grids*, i.e., orthogonally intersecting patterns of streets, (2) *colliding grids*, i.e., multiple intersecting regular grids rotated with respect to one another, (3) *curvilinear grids*, i.e., intersecting patterns of curvilinear streets, (4) *cul-de-sacs*, i.e., hierarchically branching street networks, and (5) *supergrids*, i.e., sparsely spaced orthogonally intersecting main arteries with irregular street patters (i.e., either no specific pattern or a combination of the four previous network types) filling in the large blocks surrounded by the arteries. For more information on stimuli and how they were selected, see (Christova et al. 2012).

Four stimuli per street network type (all together 20 stimuli, Fig. 1) were presented to each subject in a pseudorandom sequence.

Task

A trial started with the subjects fixating in an open circle presented at the center of a black screen and positioning an *x*–*y* joystick cursor inside the circle using their right hand. After 1.5 s, the stimulus appeared and subjects were asked to choose a hypothetical City Hall location by moving the joystick and clicking in the desired location. The subjects were instructed not to trace the path with the joystick, and the experiment proceeded at the subjects' pace (Fig. 2).

Experimental setup

Task stimuli were generated by a computer and were presented on a display 62 cm in front of the subjects, using a liquid crystal display (LCD) projector and a periscopic mirror system. The stimuli displayed subtended approximately 24 degrees of visual angle. Subjects lay supine in the recording chamber having their head inside the cryogenic helmet-shaped dewar. During the task, subjects were using a 2D joystick (joystick model: 541 FP, Measurement Systems, Norwalk, CT; remodeled by removing all the magnetic parts). The joystick was placed on the resting bed, next to subjects' right hand.

Data acquisition

The visual stimuli, the online behavioral control, and feedback were implemented in Visual Basic (Microsoft Visual Basic 2005, version 8.0). Relevant data include the times of presentation of stimuli, the *x*–*y* position of the joystick (updated at 200 Hz and collected at 1017 Hz), the *x*–*y* position of the eyes (updated at 60 Hz and collected at 1017 Hz), and the MEG signals from 248 sensors (collected at 1017 Hz). The eye position was recorded using a nonmagnetic video-based pupil/corneal reflection tracing.

Magnetoencephalography (MEG)

Brain activity was recorded using a 248-sensor whole-head axial MEG system (Magnes 3600 WH, 4-D Neuroimaging, San Diego, CA) (Fig. 3). The cryogenic helmet-shaped dewar of the MEG system was located inside a shielded room that reduced electromagnetic and environmental noise. The MEG data were recorded at 1017.25 Hz and filtered down to 0.1–400 Hz during acquisition.

Data preprocessing

The obstructive cardiac artifact was removed from the MEG data using the event-synchronous subtraction method (Leuthold 2003). MEG recordings were downsampled by averaging the MEG time series every ~16.7 ms to align them with eye position recordings. In the current study, we only used the neural data from the time that the stimulus was presented to the time that people started moving the joystick to the selected position.

Time series analysis

Neurophysiological time series often are not stationary with respect to their mean and variance and in many cases are dominated by trends which should be recognized before any analysis of correlation between time series is

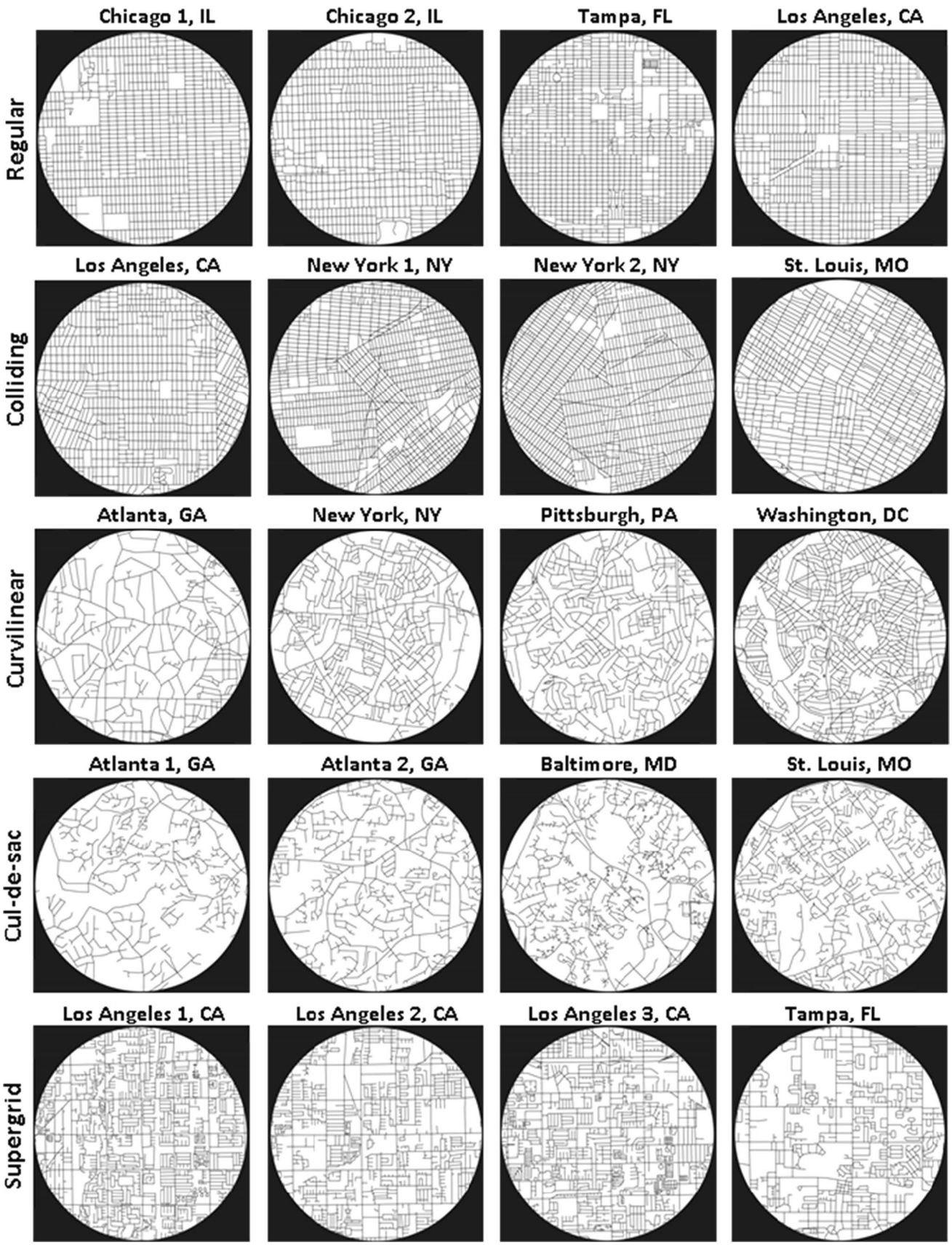

Fig. 1 Map stimuli

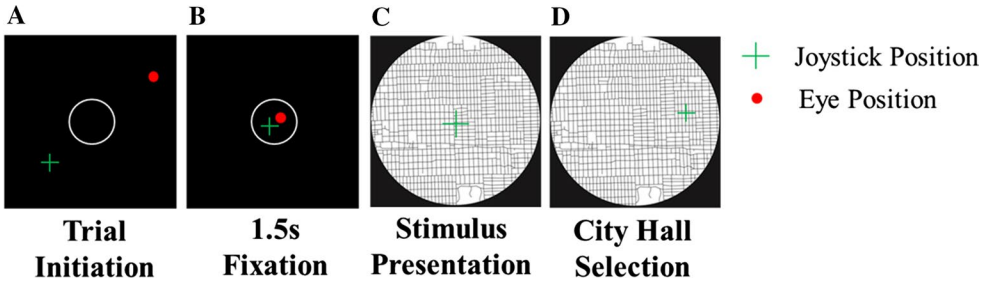

Fig. 2 Task sequence. **a** Trial starts with the presentation of an *open circle* on the *center* of a *black screen*. **b** Subject is required to fixate eyes and place the cursor of the joystick inside the *circle* for 1.5 s. **c** Stimulus is presented and subject explores the map by moving his/her eyes in order to decide where to place a hypothetical City Hall. **d** Subject chooses the City Hall location by clicking the joystick at the desired position

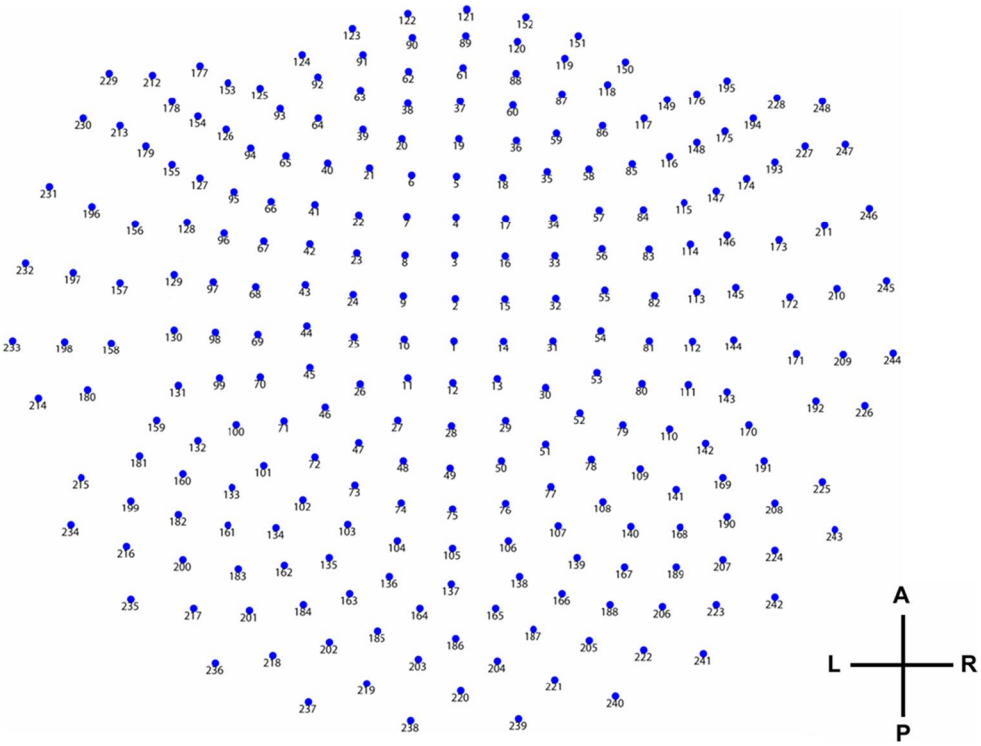

Fig. 3 2D projection of the 248-channel axial gradiometer MEG system used to record brain activity

done. Without removing nonstationarities from the data, spurious associations could arise (Leuthold et al. 2005; Box et al. 2008; Jenkins and Watts 1968). Since the main goal of this study was to assess the associations between MEG time series and map parameters, the data should be stationary. Therefore, we used an ARIMA model to render the recorded MEG data stationary and nonautocorrelated. The autoregressive (AR) model eliminates any linear dependencies (i.e., autocorrelations) within the individual time series, the integrated factor (I) differentiates the time series to remove possible linear trends, and the moving average (MA) model smoothes the time series by taking the weighted linear summation of random shocks (i.e., noise terms). Based on previous MEG studies (Leuthold et al. 2005; Langheim et al. 2006), an ARIMA(25,1,1) model was adequate to obtain quasi-stationary time series (i.e., "prewhitened" data).

Map parameters

The whole map was analyzed and characterized by the street network type (i.e., regular grid, colliding grid, curvilinear grid, cul-de-sacs, supergrid), and parts of the map defined by the circular areas of 6 DVA radius centered on each *x*–*y* eye positions, Fig. 4, were analyzed and characterized by the three space syntax attributes. The first two measures comprise the *Total Street Length* and the *Number of Street Intersections* within the circular areas of radius 6

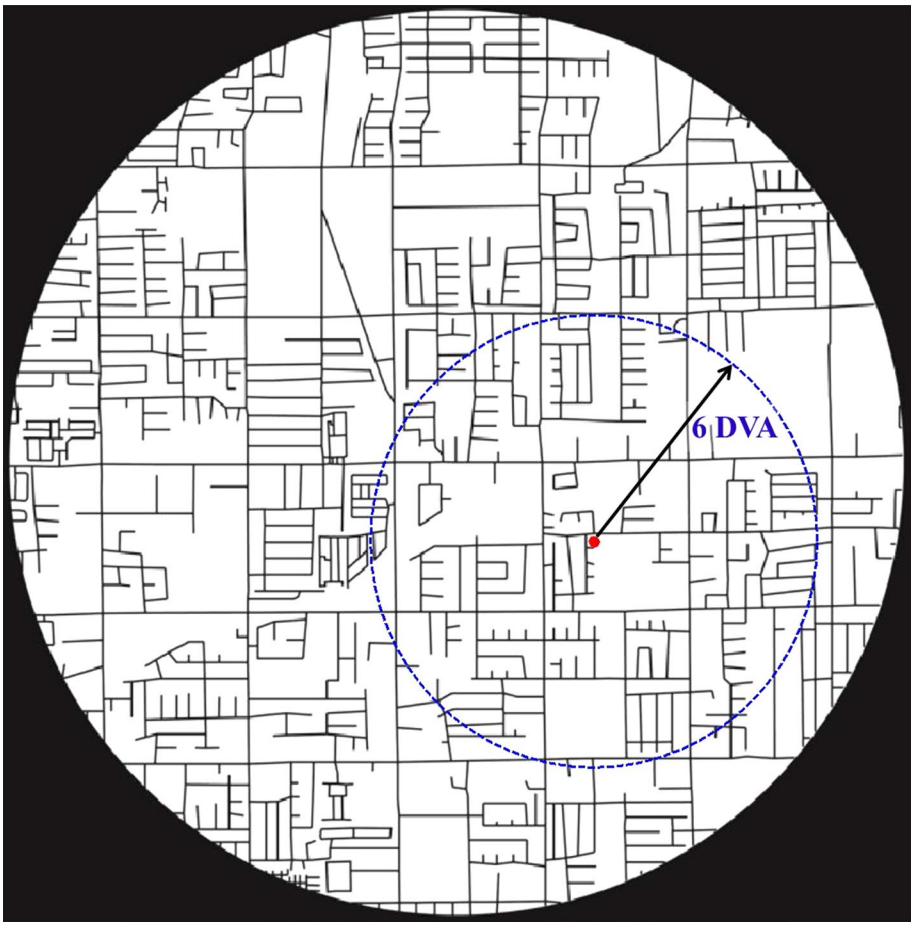

Fig. 4 Parts of the map defined by the circular areas of 6 DVA radius centered on instantaneous *x*–*y* eye positions were analyzed by space syntax characteristics. The *dot* marks an eye fixation on the map, and the *circle* corresponds to the circular area of 6 DVA radius centered on this eye position

DVA centered on instantaneous *x*–*y* eye position, normalized by the corresponding circular areas. When the *x*–*y* eye position reached near or beyond the limits of the map, these parameters were normalized using only the circular area of 6 DVA radius that lay within the map. The third measure is the *Regularity Index* within the circular areas of radius 6 DVA centered on instantaneous *x*–*y* eye positions.

Regularity index is a measure of the degree to which a given point distribution deviates from complete spatial randomness to either clustering or regularity. In a random distribution of a set of points on a given area, it is assumed that any point has had the same chance of occurring on any sub-area as any other point, that any sub-area of specified size has had the same chance of receiving a point as any other sub-area of that size, and that the placement of each point has not been influenced by that of any other point (Clark and Evans 1954).

The basis for this measure of spacing is given by the distance from an individual to its nearest neighbor, irrespective of direction. For a set of n points where the distance between the ith and the jth point is u_{ij}, the observed mean nearest neighbor distance is

$$\bar{r}_A = \frac{1}{n}\sum_{i\neq j}^{n} \min\{u_{ij}\} \tag{1}$$

In our case, the n points were the street intersections within the circular areas of 6 DVA radius centered on instantaneous *x*–y eye positions. We also calculated the mean distance to nearest neighbor that would be expected if the individuals of that population were randomly distributed. Complete spatial randomness for n points in an area A, assuming that a point is equally likely to fall at each location in the area, and that multiple points are chosen independently, is described by the Poisson process, in which the probability density function for the nearest neighbor distance d and point density $\rho = \frac{n}{A}$ (i.e., the mean number of points per unit area) is $p(d) = 2\pi\rho d e^{-\pi\rho d^2}$. The expectation of this distribution (i.e., mean distance between nearest neighbors for a random process) can be shown to have a value equal to (Clark and Evans 1954)

$$\bar{r}_E = \frac{1}{2\sqrt{\rho}}. \tag{2}$$

The ratio of the observed mean distance to the expected mean distance is the regularity index

$$R = \frac{\bar{r}_A}{\bar{r}_E}, \tag{3}$$

and serves as a measure of the degree to which the observed distribution approaches or departs from random expectation. Particularly, under this approach, clustering, randomness, and regularity are conceptualized as laying along a continuum. In a random distribution, $R = 1$. Under conditions of maximum aggregation, all points are superimposed, and therefore $R = 0$. Under conditions of maximum spacing, the points are spaced with perfect uniformity, as in triangular lattice arrangements, and R will have the value of $R = \frac{1.0746}{\sqrt{\rho}} = 2.1491$ (Clark and Evans 1954).

Analysis of the relations between neural activity and map parameters

We tested whether the ongoing neural activity is associated with some or all space syntax parameters. Therefore, we performed multiple linear regressions, one for each space syntax parameter, where the prewhitened time-varying MEG signal from 248 sensors was the dependent variable, and the independent variables were as follows: (a) a space syntax parameter time series (i.e., number of street intersections or total street length or regularity index), (b) the x-eye position time series, and (c) the y-eye position time series. However, we found that space syntax parameters and the x–y eye position time series were not stationary. Following the same procedure with neural data, we used an ARIMA model to remove the autocorrelation structure. We found that ARIMA (25,1,1) was adequate to yield quasi-stationary time series.

After all time series were rendered stationary and non-autocorrelated, we performed three multiple linear regressions, one for each space syntax parameter,

$$\begin{aligned} Y_{n\times 248} = {} & StreetIntersections_{n\times 1} a_{1\times n} + Xeye_{n\times 1} k_{1\times n} \\ & + Yeye_{n\times 1} l_{1\times n} + E_{n\times 248} \end{aligned} \tag{4}$$

$$\begin{aligned} Y_{n\times 248} = {} & StreetLength_{n\times 1} b_{1\times n} + Xeye_{n\times 1} k_{1\times n} \\ & + Yeye_{n\times 1} l_{1\times n} + E_{n\times 248} \end{aligned} \tag{5}$$

$$\begin{aligned} Y_{n\times 248} = {} & RegularityIndex_{n\times 1} c_{1\times n} + Xeye_{n\times 1} k_{1\times n} \\ & + Yeye_{n\times 1} l_{1\times n} + E_{n\times 248} \end{aligned} \tag{6}$$

Y is the dependent variable matrix with columns consisting of the 248 MEG prewhitened time series of size n. *StreetIntersections*, *StreetLength*, *RegularityIndex*, *Xeye*, and *Yeye* are the prewhitened independent variables time series and a, b, c, k, and l the corresponding regression coefficients. Finally, E is the error matrix.

To also assess whether the neural processing of space syntax parameters is modulated by the type of street network, we performed the same regressions, Eq. (4)–(6) for each street network layout, i.e., regular, colliding, curvilinear, cul-de-sac, and supergrid.

The relations of the brain signals with the space syntax parameters were quantified and summarized using the absolute t values corresponding to the regression coefficients of the regressions, Eq. (4)–(6). The absolute value of the regression coefficient indicates the strength of the relation, whereas its associated t value (i.e., ratio of the mean regression sum of squares divided by the mean error sum of squares) is a measure of the significance of the regression.

Comparison of the brain maps

Overall, the MLR analyses revealed significant relations between the ongoing MEG activity and space syntax parameters. We were interested in comparing the neural processing of these parameters between street network layouts, in other words, to get a measure of how similar two spatial distributions are, particularly, the spatial distributions in the MEG sensor space of the t values corresponding to a space syntax parameter for two different grids. We calculated the root-mean-square (RMS) value of the difference between the absolute t values corresponding to a space syntax parameter k for each pair of grids (i, j).

$$\mathrm{RMS}_k(\mathrm{grid} = i,\ \mathrm{grid} = j) = \sqrt{\frac{\sum_{s=1}^{248} \left(|t\mathrm{val}_{i,s}| - |t\mathrm{val}_{j,s}|\right)^2}{248}} \tag{7}$$

where k corresponds to a space syntax parameter (i.e., number of street intersections, total street length, and regularity index), grid is the street network type (i.e., regular, colliding, curvilinear, cul-de-sac, and supergrid), and s is the MEG sensor number. RMS_k is a 5×5 distance matrix, with entry (i, j) corresponding to the "similarity" of the spatial distributions in the sensor space of the t values for space syntax parameter k between grids i and j. When RMS_k (i, j) goes to zero, then the two brain maps have about the same spatial distributions, suggesting that the same brain networks are involved in processing the space syntax parameter k for grids i and j.

Distances between objects can be visualized in many simple and evocative ways. Here, we are considering a graphical representation of a matrix of distances or dissimilarities (in our case the RMS matrix) with a dendrogram or a tree, where the objects are clustered together in a hierarchical fashion from the closest, that is most similar, to the furthest apart, that is the most different. In the dendrogram, clusters are distanced from an origin according to a scaling

factor starting at distance 0 for items that are approximately equal and ending at distance 25 for items that are very different. Therefore, the further from the origin a cluster forms, the less alike they can be considered.

Results

Exploration time

We calculated the time between the stimulus onset to the subjects' response to measure how fast the subjects explored the maps to decide where to place the City Hall. We found that subjects made a decision within 6.94 ± 0.44 s (mean ± SEM, $N = 200$ trials). We performed an ANOVA to assess the effects of street network type on exploration time using the subjects as a random factor. The results showed that the exploration time did not depend on the street network type (F test, $P = 0.1146$). Figure 5 shows the mean exploration time across subjects for each grid. Although there were no significant effects of the grid on the exploration time, there was orderly increase in the exploration time with respect to the grid.

Map parameters

While exploring the maps, subjects fixated at various locations. For each x–y eye position, we computed three space syntax parameters (i.e., number of street intersections, total street length and regularity index) that describe locally the map. The mean value across subjects of the space syntax parameters for each street network type is shown in Fig. 6. Note that for the same street network type the variability of space syntax parameters among subjects is low. However, space syntax parameters vary significantly across grids ($P < 0.001$).

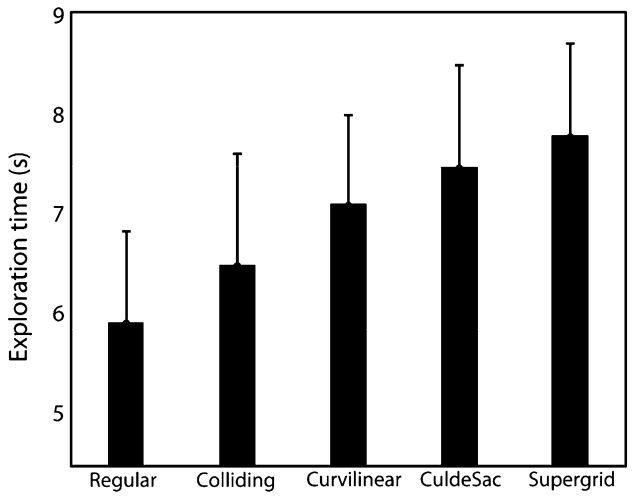

Fig. 5 Mean ± SEM of the exploration time (i.e., time from the stimulus onset to response) across ten subjects for each street network type

Relation between neural activity and map parameters

To look at the relationship between the ongoing neural activity and space syntax parameters, we performed MLR analyses to regress the MEG time series on each of the space syntax parameters, Eq. (4)–(6). We then used the absolute t values ($P < 0.05$) corresponding to the regression coefficients to get a measure of the significance of the relations. Results revealed statistically significant relations between the ongoing neural activity and space syntax parameters. Figure 7 illustrates the spatial distributions of the 248 MEG sensors involved in the processing of space syntax parameters. Red color indicates sensors highly associated with the processing of a space syntax parameter, whereas blue indicates sensors that are not involved in space syntax processing. Interestingly, there is a strong focus of space syntax sensors in the right frontal cortex. Particularly, processing of total street length and regularity index involved predominantly right frontal and prefrontal areas (Fig. 7b, c). With respect to the regularity index, there is also a strong focus on cerebellum and right temporal cortex, (Fig. 7c). Finally, processing of number of street intersections revealed patches mainly in prefrontal areas (Fig. 7a). The brain areas were estimated based on a 3D sensory layout in the MEG helmet and typical brain reconstruction from brain MRIs using the integrated BESA (version 5.06, MEGIS Software GmbH, Gräfelfing, Germany) and Brain Voyager (Electrical Geodesics, Inc., Eugene OR, USA) package.

It should be noted that in this and subsequent figures (Figs. 7, 8, 9, 10), we illustrate the 2D contour plots in the MEG sensor space of the mean absolute t values across ten subjects using $P < 0.05$ as a floor threshold. We did not correct for multiple comparisons (for 248 sensors) since the ultimate goal of the study is to show the brain maps that have high and low associations with the space syntax parameters. So, even sensors with uncorrected P value close to 0.05 are necessary to be represented in the brain map to evaluate the differences among areas in their strength of associations with specific space syntax parameters. Nevertheless, the following considerations apply, at face value, to this issue of multiple comparisons. In our multiple regression analyses involving time series, the degrees of freedom for the t statistic related to a regression coefficient exceeded 6000 in all analyses, since all subjects were included in any specific MLR (e.g., per grid). The nominal (uncorrected) P value of 0.05 for 248 multiple comparisons corresponds to a Bonferroni-corrected P value of $0.05/248 = 0.0002$.

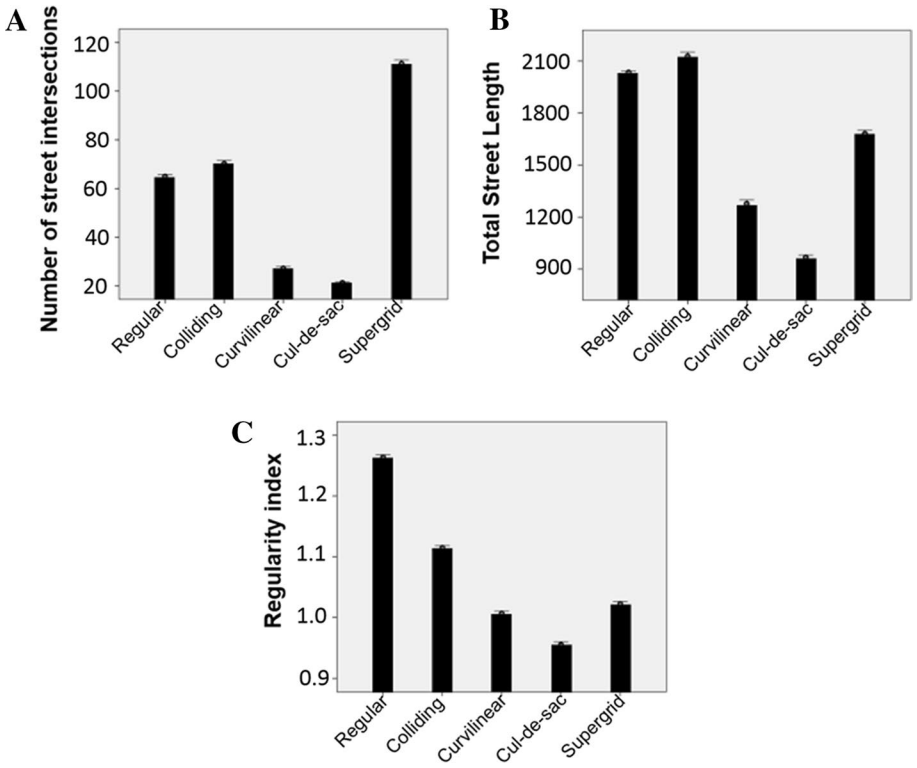

Fig. 6 Mean ± SEM of the **a** number of street intersections, **b** total street length, and **c** regularity index, across ten subjects for each street network type

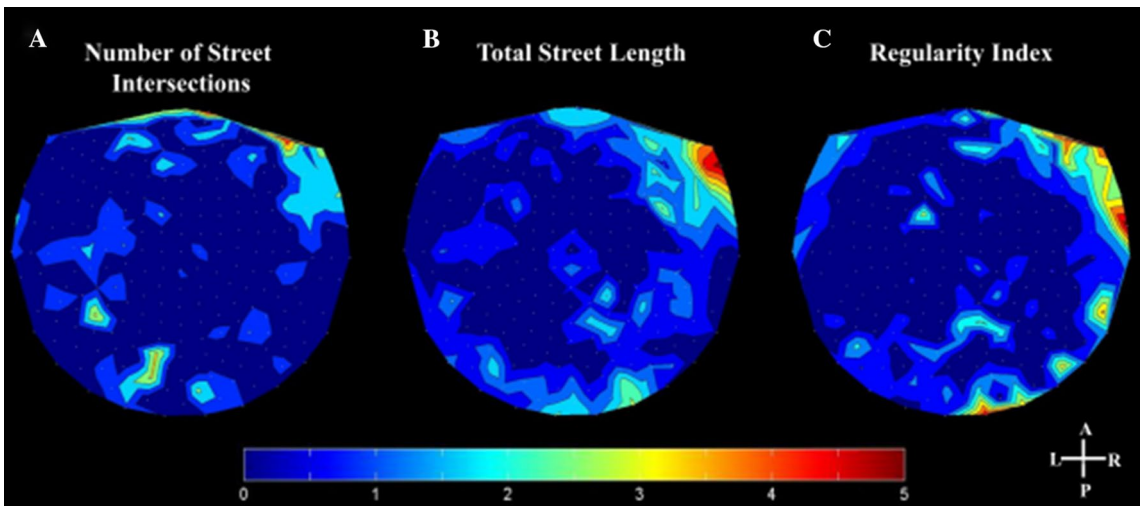

Fig. 7 Spatial distributions of the neural processing of **a** number of street intersections, **b** total street length, and **c** regularity index, across all street network types. 2D contour plots in the MEG sensor space of the mean absolute t values ($P < 0.05$) across ten subjects corresponding to the regression coefficients of space syntax parameters in the linear regressions, Eq. (4)–(6)

Now, it can be seen in Figs. 7, 8, 9, and 10 that the t values for the (limited) hot spots in the contour maps were at least $t = 5$ and up to $t = 7$. The corresponding nominal (uncorrected) P values are $P = 5.89 \times 10^{-7}$ (for $t = 5$) and $P = 2.8 \times 10^{-12}$ (for $t = 7$). Therefore, the hotspots in the maps are way above the (corrected) $P = 0.05$ value of 0.0002.

These findings raised the question of whether the neural processing of space syntax parameters differs between street network layouts. To address this question, we performed *for each grid* the same regression analysis. Figures 8, 9, and 10 illustrate the spatial distributions of the sensors involved in the processing of number of street intersections, total street length, and regularity

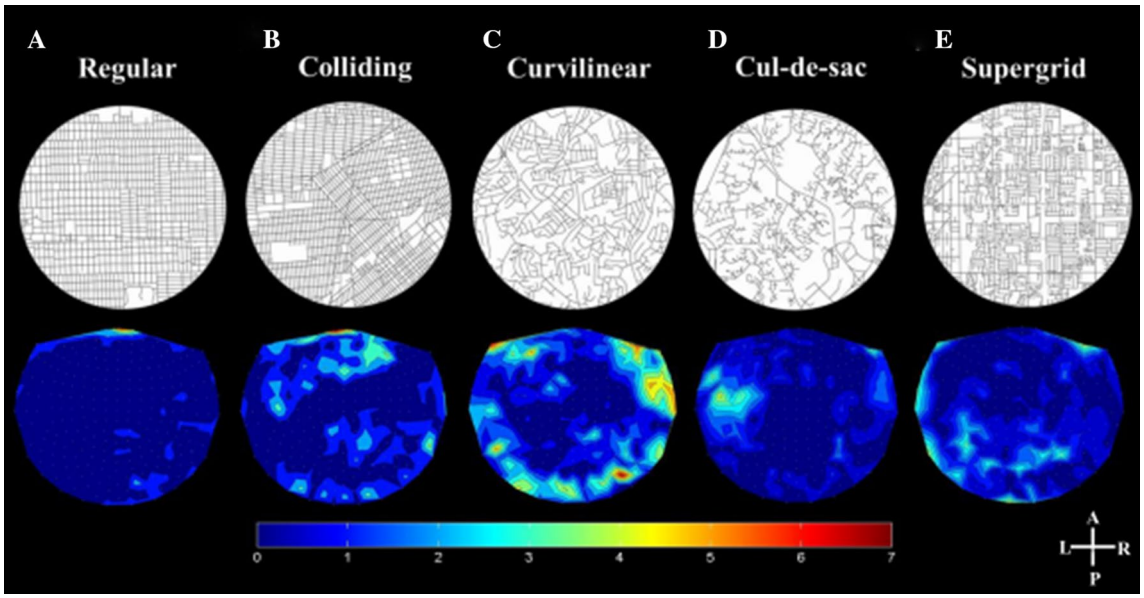

Fig. 8 Spatial distributions of the neural processing of the *number of street intersections* for each street network type. *First row* illustrates example stimuli from **a** regular, **b** colliding, **c** curvilinear, **d** cul-de-sac, and **e** supergrid street network layouts. *Second row* illustrates 2D contour plots in the MEG sensor space of the mean absolute *t* values across ten subjects ($P < 0.05$) corresponding to the regression coefficients of number of street intersections in the linear regressions for each street network type, respectively, Eq. (4)

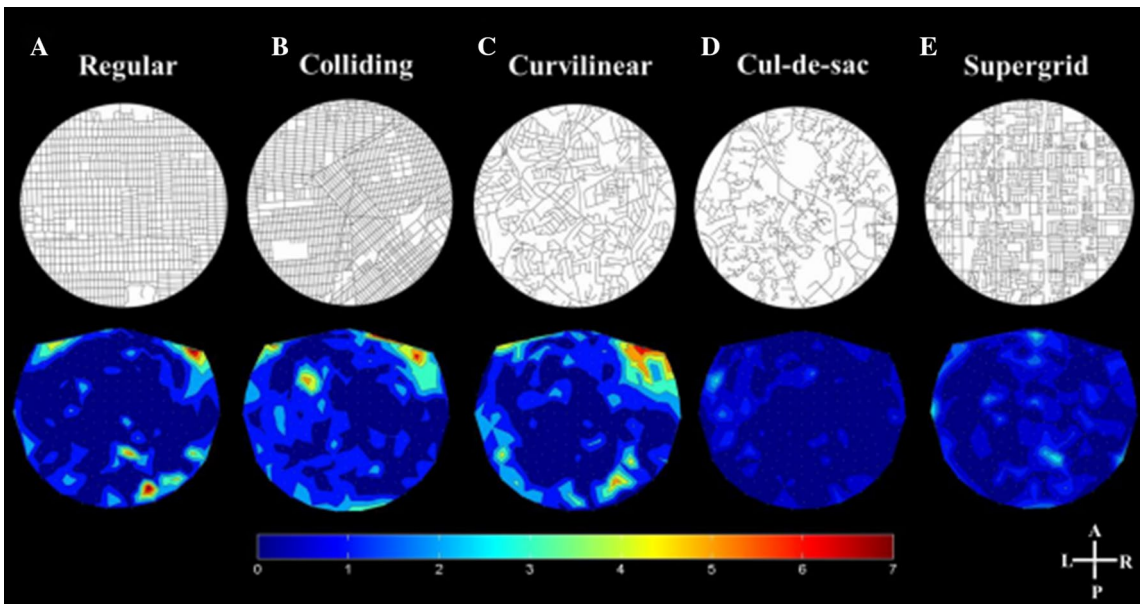

Fig. 9 Spatial distributions of the neural processing of the *total street length* for each street network type. *First row* illustrates example stimuli from **a** regular, **b** colliding, **c** curvilinear, **d** cul-de-sac, and **e** supergrid street network layouts. *Second row* illustrates 2D contour plots in the MEG sensor space of the mean absolute *t* values across ten subjects ($P < 0.05$) corresponding to the regression coefficients of total street length in the linear regressions for each street network type, respectively, Eq. (5)

index, respectively, for each street network type. There are several interesting findings. Overall, processing of the number of street intersections and the total street length involved mainly right frontal and prefrontal areas for regular, colliding, and curvilinear street network layouts (Figs. 8, 9a–c). However, cul-de-sacs and supergrids involved minimal processing of these space syntax characteristics (Figs. 8, 9d, e).

Particularly, with respect to the number of street intersections (Fig. 8), there was a strong focus around OFC for

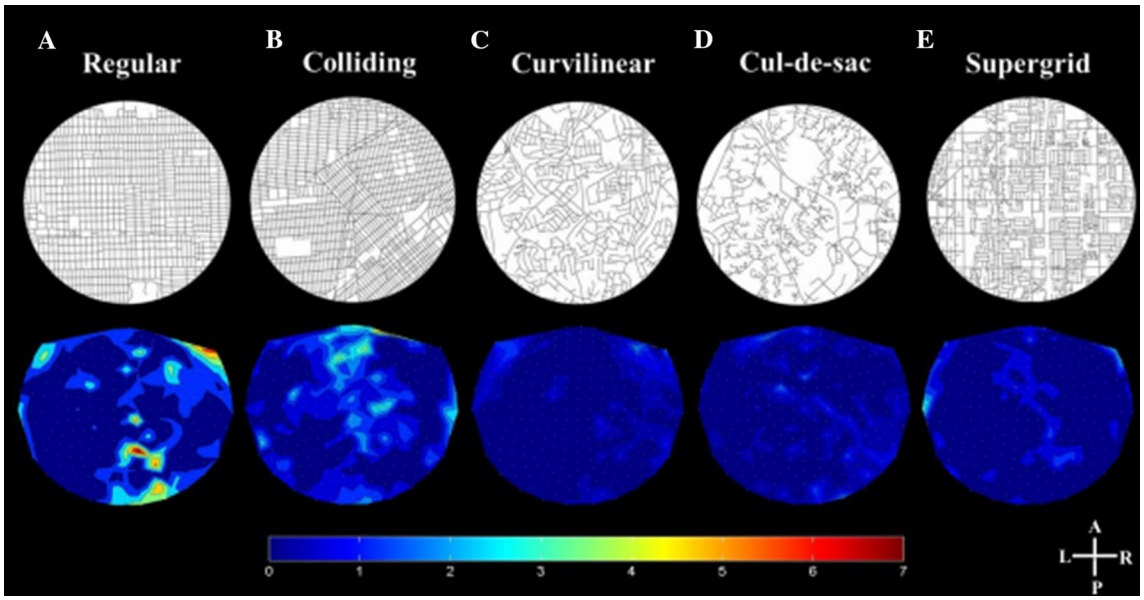

Fig. 10 Spatial distributions of the neural processing of the *regularity index* for each street network type. *First row* illustrates example stimuli from **a** regular, **b** colliding, **c** curvilinear, **d** cul-de-sac, and **e** supergrid street network layouts. *Second row* illustrates 2D contour plots in the MEG sensor space of the mean absolute *t* values across ten subjects ($P < 0.05$) corresponding to the regression coefficients of regularity index in the linear regressions for each street network type, respectively, Eq. (6)

Table 1 Summary of the brain maps in Figs. 8, 9, and 10

	Regular	Colliding	Curvilinear	Cul-de-sac	Supergrid
Street intersections	Prefrontal (around OFC)	Prefrontal (around OFC)	Bilateral prefrontal Right frontal–temporal Cerebellum	Minimal processing (No specific areas)	Minimal processing (No specific areas)
Total street length	Right prefrontal Parieto-occipital Cerebellum	Right prefrontal	Right prefrontal Cerebellum	Minimal processing (No specific areas)	Minimal processing (No specific areas)
Regularity index	Right prefrontal Parieto-occipital	Prefrontal (minimal processing)	Minimal processing (No specific areas)	Minimal processing (No specific areas)	Minimal processing (No specific areas)

Estimates of the brain areas involved in the neural processing of the number of street intersections, the total street length, and the regularity index

regular (panel A) and colliding grids (panel B) and on bilateral prefrontal, right frontal–temporal, and cerebellar areas for curvilinear grids (panel C). Processing of total street length for regular street networks mainly involved right prefrontal, cerebellar, and parieto-occipital cortex (Fig. 9a). For colliding grids, total street length sensors were focused mainly on right prefrontal and secondarily on left frontal cortex (Fig. 9b), whereas for curvilinear grids, they were localized on right prefrontal and cerebellar areas (Fig. 9c). Finally, with respect to the regularity index (Fig. 10), there was a strong focus on right prefrontal and parieto-occipital areas for regular grids (panel A). Colliding street networks involved minimal processing of regularity index, associated with prefrontal areas (panel B). For cul-de-sacs (panel D), supergrids (panel E), and curvilinear grids (panel C), the association of regularity index with neural signal was minimal. Table 1 summarizes the brain maps in Figs. 8, 9, and 10.

We then used hierarchical cluster analysis to map changes in the neural processing of a space syntax parameter for different types of street networks. This method clusters the spatial distributions of the sensors involved in the processing of a space syntax parameter for each street network type, according to a similarity measure. Similarity of the neural processing of a space syntax parameter between two grids was assessed by computing the RMS value of the difference between the absolute *t* values corresponding to this space syntax parameter of the two grids, Eq. (7) (see "Materials and methods" section). Street network types included in the same cluster, then, can be judged to involve

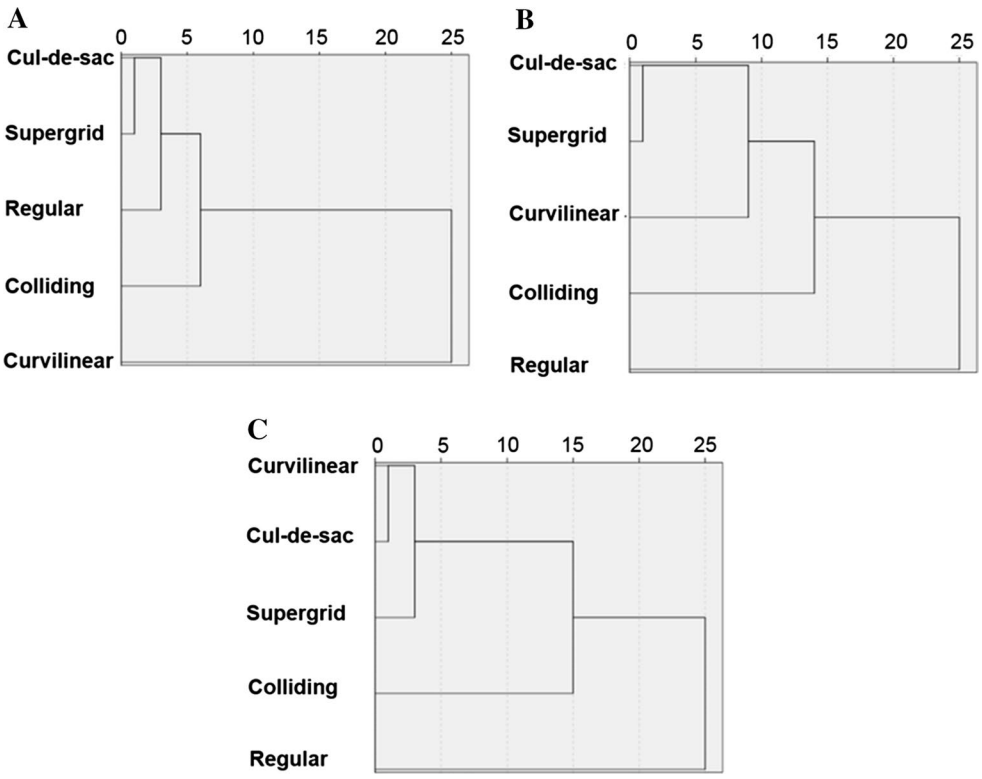

Fig. 11 Dendrograms (using the average linkage between groups) displaying the clusters resulting by joining the grids that are most similar, in terms of their spatial distributions in the MEG sensor space of the absolute *t* values corresponding to **a** the number of street intersections, **b** the total street length, and **c** the regularity index

similar neural processing of a space syntax parameter. The results of hierarchical tree clustering are summarized by dendrograms, which indicate at what level of similarity any two clusters were joined. With respect to the number of street intersections (Fig. 11a), cul-de-sac and supergrid are the most similar and join to form the first cluster. Note that they were both minimally involved in the neural processing of number of street intersections (see Fig. 8d, e). Then, regular grid joined to form the second cluster, followed by the joining of colliding grid at distance 6. Finally, curvilinear grid merged at distance 25, indicating neural processing that differs from the other street network types. This is true, since the sensors associated with number of street intersections for curvilinear grids were more widely distributed than the ones for the rest street network layouts (see Fig. 8c). Similarly, with respect to the total street length (Fig. 11b), cul-de-sac and supergrid merged at close distance to form the first cluster, followed by the joining of curvilinear grid, at distance 9. Colliding grid joined at distance 14, and regular grid merged at distance 25. Long distances between clusters indicate the dissimilarity in the neural processing of total street length between different street network types. Finally, for the neural processing of regularity index (Fig. 11c), curvilinear, cul-de-sac, and supergrid merged in the same cluster at distance 3, since they involve minimal processing of this parameter (see Fig. 10c–e). Colliding grid joined at distance 15, followed by regular at distance 25. Note that neural processing of regularity index was involved mainly in regular and secondarily in colliding grid (see Fig. 9a, b).

Discussion

In recent years, scientists have made significant progress in understanding the neural basis of decision making. The vast majority of these studies have heavily focused on economic decisions, in which the main question is how the brain computes, represents, and compares values of alternative items/goods to select the best alternative. According to these studies, the brain integrates all the decision variables related with an option (e.g., price, quality, brand) into a single value that characterizes the subjective value of this option (Padoa-Schioppa and Assad 2006; Padoa-Schioppa 2007, 2011). Decision is made after comparing the subjective values of available options to find the best alternative. The main characteristic in economic choices is that subjective values depend on the options themselves. While economic choice is an important component of human behavior, people frequently have to select between options whose values are strongly dependent on the spatial characteristics of the environment. It is also likely that the values are not immediately evident before exploring and/or navigating within the environment where the alternatives are located. For instance, when looking for a new house, the values of the alternative options depend also on the spatial

characteristics of the areas that houses are located, such as distance from work and accessibility to highways. Evaluating these characteristics may involve map exploration and/or navigation around these areas. How the brain represents and processes spatial information acquired during exploration to make decisions is still poorly understood.

In the current study, we conducted a novel brain imaging experiment to test the hypothesis that a network of cortical regions is involved in the processing of spatial information acquired during exploration to make a decision. We recruited 10 subjects and asked them to explore small city maps exemplifying five different street network types (i.e., regular, colliding, curvilinear, cul-de-sac, and supergrid) to build a hypothetical City Hall, while neuronal activity was recorded continuously by 248 MEG sensors at high temporal resolution. We also monitored subjects' eye positions to locally characterize the maps by computing three space syntax parameters within the circular areas of 6 DVA radius centered on each eye position ("eye's mind"): a) total street length, b) number of street intersections, and c) regularity index. After preprocessing both MEG time series and space syntax parameters time series to render stationary data, we performed an MLR analysis to regress the time-varying MEG signal from the 248 sensors on each of the space syntax parameters.

In line with our hypothesis, we found that ongoing neural activity was strongly associated with space syntax parameters through localized and distributed networks. Interestingly, right frontal and prefrontal areas were predominantly involved in the processing of all space syntax parameters. Even though this finding is somehow counterintuitive since higher cognitive brain regions have long been associated with the evaluation/comparison of values in economic choices (O'Doherty 2011), recent studies in rodents suggest that frontal areas encode also spatial variables needed to define specific behavioral goals in navigation and way-finding tasks (Feierstein et al. 2006). Another possible scenario is that these parameters were used for the evaluation of different locations in the map.

It is likely that when subjects fixated to a particular location, they used these (and probably others) spatial parameters to evaluate the "attractiveness" of this location and to compare it with other alternatives. In that way, these spatial characteristics can be considered as decision variables that characterize the value of a location, and therefore, they are encoded in the frontal areas of the brain.

Additionally, neural processing of the regularity index also involved right temporal and cerebellar areas. It has been suggested that temporal areas, such as inferior temporal cortex (IT), encode the position of different objects presented in a scene (Aggelopoulos and Rolls 2005). The regularity index in a broad sense characterizes the relative positions between the street intersections (i.e., it measures the degree to which the distribution of street intersections deviates from complete spatial randomness to either clustering or regularity), and so, it may be encoded by IT. The cerebellum has long been exclusively associated with motor control and high cognitive functions, such as attention (Veneri et al. 2014). However, recent studies provide evidence that it also participates in spatial information processing. In particular, behavioral and neurophysiological studies in cerebellar mutant mice showed that the cerebellum interacts and communicates with the hippocampus to participate in the construction of the "cognitive map" (for review see Rochefort et al. 2013). In terms of the anatomical connection between these two regions, although a direct cerebello-hippocampal projection has been suggested, recent findings argue against this theory suggesting a multisynaptic pathway involving posterior parietal cortex and retrosplenial cortices (Prevosto et al. 2010; Rochefort et al. 2013).

It could be argued that the associations between neural activity and space syntax parameters reflect eye movements. One way to deal with this issue is to use EOG information as covariates to the regression analysis. Since we did not record EOG activity in this study, we used the *x*–*y* eye positions as covariates in the regression analysis to ensure that the associations between MEG activity and map parameters do not reflect eye movements. Additionally, these associations are not due to the locations of the receptive visual fields mapped outside the space syntax context of map exploration, in that receptive field centers and space syntax characteristics were not spatially distinguishable.

Our findings raised the question of whether the processing of space syntax parameters differs among the five street network types. To address this question, we performed the same regression analyses, but now for each street network type. Using clustering analysis, we found differences on the neural processing of the space syntax parameters between the five different street network types. In particular, the results showed that neural processing of the number of street intersections and total street length mainly involved frontal and prefrontal areas, but only for regular, colliding, and curvilinear grids. Instead, cul-de-sacs and supergrids involved minimal processing of these two space syntax parameters. These findings suggest that the number of street intersections and total street length are important spatial features for deciding among many options where to build the hypothetical City Hall, but only for regular, colliding, and curvilinear street network types. On the contrary, people seem to ignore these parameters when exploring cul-de-sacs and supergrids, suggesting that they may use other kinds of information (e.g., curvature) to make a decision. Regarding the regularity index, there was a strong focus on right prefrontal and parieto-occipital areas for regular grids and a weaker focus on prefrontal cortex

for colliding grids. On the other hand, there was minimal or no processing of the regularity index for cul-de-sacs, supergrids, and curvilinear grids. Based on these findings, regularity index seems to be an important spatial characteristic for the evaluation of the alternative locations to find the best place for the hypothetical City Hall, but only for regular and colliding grids. This is also in line with the fact that the regularity index is significantly higher for regular and colliding grids compared to the rest of the street network types.

Overall, we presented a novel brain imaging study to assess the relation between neural activity and particular space syntax parameters. The results complement behavioral findings from a series of previous studies, suggesting that people use spatial characteristics of the environment to make decisions. To the best of our knowledge, this is the first study showing that spatial information required to make decisions is encoded through localized and distributed brain areas. These results suggest new avenues to elucidate the neural basis of spatial information processing in exploration and decision making.

Acknowledgments This work was supported by the McKnight Presidential Chair in Cognitive Neuroscience, University of Minnesota (A.P.G.).

References

Aggelopoulos N, Rolls E (2005) Scene perception: inferior temporal cortex neurons encode the positions of different objects in the scene. Eur J Neurosci 22:2903–2916

Aguirre GK, Detre JA, Alsop DC, D'Esposito M (1996) The parahippocampus subserves topographical learning in man. Cereb Cortex 6:823–829

Box G, Jenkins G, Reinsel G (2008) Time series analysis: forecasting and control, 4th edn. Wiley, Hoboken

Chafee M, Averbeck B, Crowe D, Georgopoulos AP (2002) Impact of path parameters on maze solution time. Arch Ital Biol 140:247251

Christova P, Scoppa M, Peponis J, Georgopoulos AP (2012) Exploring small city maps. Exp Brain Res 223(2):207–217. doi:10.1007/s00221-012-3252-z

Clark P, Evans F (1954) Distance to nearest neighbor as a measure of spatial relationships in populations. Ecology 35:445–453

Crowe D, Averbeck B, Chafee M, Anderson J, Georgopoulos AP (2000) Mental maze solving. J Cogn Neurosci 12:813–827

Feierstein C, Quirk M, Uchida N, Sosulski D, Mainen Z (2006) Representation of spatial goals in rat orbitofrontal cortex. Neuron 51:495–507

Hillier B (1996) Space is the machine. Cambridge University Press, Cambridge

Jenkins GM, Watts DG (1968) Spectral analysis and its applications. Holden-Day, Oakland

Langheim FJ, Leuthold AC, Georgopoulos AP (2006) Synchronous dynamic brain networks revealed by magnetoencephalography. Proc Natl Acad Sci USA 103:455–459. doi:10.1073/pnas.0509623102

Leuthold AC (2003) Subtraction of heart artifact from MEG data: the matched filter revisited. 33rd Annual Meeting of the Society for Neuroscience. New Orleans, LA, 8–12 November. 863.15

Leuthold AC, Langheim FJ, Lewis SM, Georgopoulos AP (2005) Time series analysis of magnetoencephalographic data during copying. Exp Brain Res 164:411–422. doi:10.1007/s00221-005-2259-0

Maguire E, Frackowiak R, Frith C (1998) Recalling routes around london: activation of the right hippocampus in taxi drivers. J Neuroscience 17:7103–7110

O'Doherty J (2011) Contribution of the ventromedial prefrontal cortex to goal-directed action selection. Ann N Y Acad Sci 1239:118–129

Padoa-Schioppa C (2007) Orbitofrontal cortex and the computation of economic value. Ann N Y Acad Sci 1121:232–253

Padoa-Schioppa C (2011) Neurobiology of economic choice: a good-based model. Annu Rev Neurosci 34:333–359

Padoa-Schioppa C, Assad J (2006) Neurons in orbitofrontal cortex encode economic value. Nature 44:223–226

Peponis J, Wineman J (2002) Spatial structure of environment and behavior. In: Bechtel RB, Churchman A (eds) Handbook of environmental psychology, 2nd edn. Wiley, New York, NY

Prevosto V, Graf W, Ugolini G (2010) Cerebellar inputs to intraparietal cortex areas lip and mip: functional frameworks for adaptive control of eye movements, reaching, and arm/eye/head movement coordination. Cereb Cortex 20:214–228

Rochefort C, Lefort J, Rondi-Reig L (2013) The cerebellum: a new key structure in the navigation system. Front Neural Circuits 7:1–12

Spiers H, Maguire E (2006) Thoughts, behaviour, and brain dynamics during navigation in the real world. Neuroimage 31:1826–1840

Spiers H, Maguire E (2007) A navigational guidance system in the human brain. Hippocampus 17:618–626

Veneri G, Federico A, Rufa A (2014) Evaluating the influence of motor control on selective attention through a stochastic model: the paradigm of motor control dysfunction in cerebellar patient. Biomed Res Int 2014:1–13